VIP High-Pressure NMR Spectroscopy | Very Important Paper

DOI: 10.1002/anie.201404994

A High-Pressure NMR Probe for Aqueous Geochemistry**

*Brent G. Pautler, Christopher A. Colla, Rene L. Johnson, Peter Klavins, Stephen J. Harley, C. André Ohlin, Dimitri A. Sverjensky, Jeffrey H. Walton, and William H. Casey**

Abstract: *A non-magnetic piston-cylinder pressure cell is presented for solution-state NMR spectroscopy at geochemical pressures. The probe has been calibrated up to 20 kbar using in situ ruby fluorescence and allows for the measurement of pressure dependencies of a wide variety of NMR-active nuclei with as little as 10 μL of sample in a microcoil. Initial ^{11}B NMR spectroscopy of the H_3BO_3–catechol equilibria reveals a large pressure-driven exchange rate and a negative pressure-dependent activation volume, reflecting increased solvation and electrostriction upon boron-catecholate formation. The inexpensive probe design doubles the current pressure range available for solution NMR spectroscopy and is particularly important to advance the field of aqueous geochemistry.*

The reactivity and speciation of elements under extreme conditions is the essence of geochemistry. Aqueous geochemical calculations employing Helgeson–Kirkham–Flowers (HKF) equations of state are used to quantify molecular reactions based on their equilibrium constants in hydrothermal systems, such as within the Earth's crust.[1] Recently, these equations have been expanded up to 1200 °C and 60 kbar using new estimates of the dielectric properties of water.[2,3] These predictions aid in the analysis of water–rock interactions but are restricted to a limited number of molecular species as few spectroscopic techniques are available to probe chemical speciation under high-pressure conditions. Experimental validation of these speciation predictions has largely been limited to a 5 kbar pressure maximum.

Aqueous geochemical reactions involving aluminium,[4] silicates,[5–7] magnesium,[7,8] carbonates,[9] sulfur,[10] and boron[11] have been examined experimentally in situ via diamond-anvil cells coupled to Raman spectroscopy in an attempt to extract thermodynamic properties. New species are often inferred from slight changes to the broad band-stretching frequencies. The development of a new high-pressure containment technique for aqueous solutions would allow for the acquisition of high-resolution molecular data.

At ambient conditions, NMR spectroscopy has emerged as a powerful analytical technique to monitor chemical processes within the environment.[12] Furthermore, advancements in high-resolution, high-pressure probe design[13–15] have not only allowed for the study of geochemical reaction dynamics,[16–18] but also the pressure dependencies of critical micelle concentrations,[19] dissolved gas formation from catalytic reactions,[20] as well as several studies probing protein folding, aggregation, and stabilization of rare high-energy states.[21–24] Despite the tremendous scientific advancement from these studies, the current NMR probe designs cannot fully accommodate both high pressures and high-resolution molecular-level data needed to begin to evaluate the geochemical models.

Advances in condensed-matter physics led to the development of non-magnetic piston-cylinder pressure cells that are capable of achieving 35 kbar at room temperature.[25] This clamp-cell design (see Supporting Information Figure SI 1 for a photo) allows for pressure to be increased by an external hydraulic press and held by a locknut. The cell is machined from beryllium-copper (BeCu) and is fitted with a tuneable (single or double) resonant circuit with a microcoil designed to fit inside the cell and subsequently pressurized.[25] The pressure clamp design fits inside a standard wide-bore NMR magnet, with the temperature controlled externally by a water bath. The three-turn solenoid microcoil (Figure 1, inset) is constructed as a part of the electrical feedthrough, and secured with Stycast 2850FT epoxy mixed with a small amount of Al_2O_3 powder to seal the pressure. Upon assembly, as outlined by Walker,[25] the probe can be tuned to the desired Larmor frequency by adjusting the overall capacitance or inductance. The pressure inside the cell is easily determined and calibrated via in situ ruby fluorescence where

[*] Dr. B. G. Pautler, Dr. R. L. Johnson, Prof. W. H. Casey
Department of Chemistry, University of California, Davis
1 Shields Ave, Davis, CA 95616 (USA)
E-mail: whcasey@ucdavis.edu
C. A. Colla, Prof. W. H. Casey
Department of Earth and Planetary Sciences
University of California, Davis (USA)
P. Klavins
Department of Physics
University of California, Davis (USA)
Dr. J. H. Walton
NMR Facility, University of California, Davis (USA)
Dr. S. J. Harley
Energetic Materials Division
Lawrence Livermore National Laboratory
7000 East Ave. Livermore, CA 94550 (USA)
Dr. C. A. Ohlin
School of Chemistry, Monash University
Wellington Rd, Clayton VIC 3800 (Australia)
Prof. D. A. Sverjensky
Department of Earth & Planetary Sciences
Johns Hopkins University, Baltimore, MD 21218 (USA)
and
Geophysical Laboratory, Carnegie Institution of Washington
Washington, DC 20015 (USA)

[**] This work is supported by the Department of Energy grant DE-FG02-05ER15693 and by LLNL under Contract DE-AC52-07NA2734 LLNL-JRNL-654755. Additional funding sources and awknowledgements are listed in the Supporting Information.

Supporting information for this article is available on the WWW under http://dx.doi.org/10.1002/anie.201404994.

 © 2014 Wiley-VCH Verlag GmbH & Co. KGaA, Weinheim

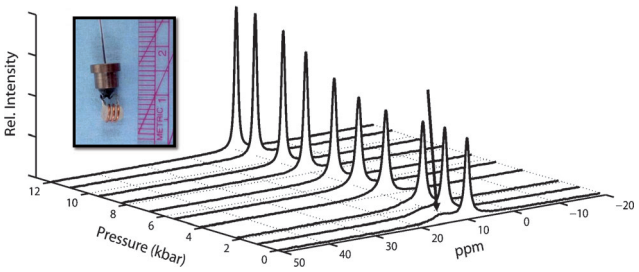

Figure 1. ^{11}B NMR spectra as a function of pressure of a $NaB(OH)_4$ solution (0.1 M) in a microcoil. The arrow highlights the broad resonance associated with polyborate species that disappears with increasing pressure while the inset shows the BeCu feedthough with 10 μL of sample in Peek tubing.

a fiber optic cable is used in the feedthrough[26] and the shift of the R1 fluorescence line monitored. The relationship between the wavelength of the ruby fluorescence and pressure,[27] allowed for the construction of calibration curves up to 20 kbar (Figure SI 2) to ensure accuracy.

The probe was tested with a well-characterized, geochemically relevant chemical system. Using the Deep Earth Water HKF model,[2] the equilibrium constant of H_3BO_3 with water is predicted to increase by eight orders of magnitude as pressure increases from ambient conditions to 20 kbar (Figure SI 3) and has been experimentally shown to increase by three orders of magnitude up to 9 kbar.[28] This change leads to a drop in solution pH and change in speciation which is easily monitored by ^{11}B NMR spectroscopy.[29] An ambient ^{11}B NMR spectrum of $NaB(OH)_{4(aq)}$ (0.1M) collected using this high-pressure probe has two resonances resulting from borate (8.9 ppm) and polyborate (14.3 ppm; highlighted with the arrow) species in solution (Figure 1).[30,31] As pressure is increased hydrostatically, the polyborate oligomer resonance decreases as the borate peak sharpens and becomes more intense, indicating that the polyborate dissociates into monomers due to the increase in pressure and volume reduction. Furthermore, the spin-lattice relaxation (T_1) and spin-spin relaxation (T_2) of a 0.05 M $H_3BO_{3(aq)}$ solution measured with this probe only varied from 8.2–7.1 ms and 3.1–5.5 ms up to 8 kbar respectively, consistent with the change in solution viscosity over this pressure range,[32] indicating that change in signal shape is due to the solution dynamics resulting from perturbations to the equilibria.

The chemistry of organic-borate complexes has been well studied at ambient conditions.[29,33] In particular, the mechanism of complexation of H_3BO_3 with catechol (Scheme 1)[34–36] has previously been studied by ^{11}B NMR spectroscopy.[37,38] The speciation depends on pH (SI 4) and may therefore react differently as a function of pressure, which generally favours increased dissociation of Brønsted acids. At ambient pressure and 40 °C, a 1:1 molar solution of H_3BO_3:catechol, adjusted to pH° 5.1 (the superscript indicates ambient pressure) with NaOH displays three ^{11}B-resonance signals at 7.4, 12.8, and 19.0 ppm corresponding to the mono-catecholate, bis-catecholate, and free H_3BO_3, respectively (Figure 2 A). As pressure is increased inside the cell, the ^{11}B NMR signals broaden and coalesce, indicating pressure-driven chemical exchange. Initially upon pressurization, the signal corresponding to the bis-catecholate species disappears, signifying that its formation is not favored at higher pressures and/or that the signal is completely broadened into the baseline by rapid interconversion. As pressure is raised from 1 to 8 kbar, the mono-catecholate and H_3BO_3 signals continue to broaden, eventually coalescing completely at 8 kbar. The coalescence is reversible upon the release of pressure (see

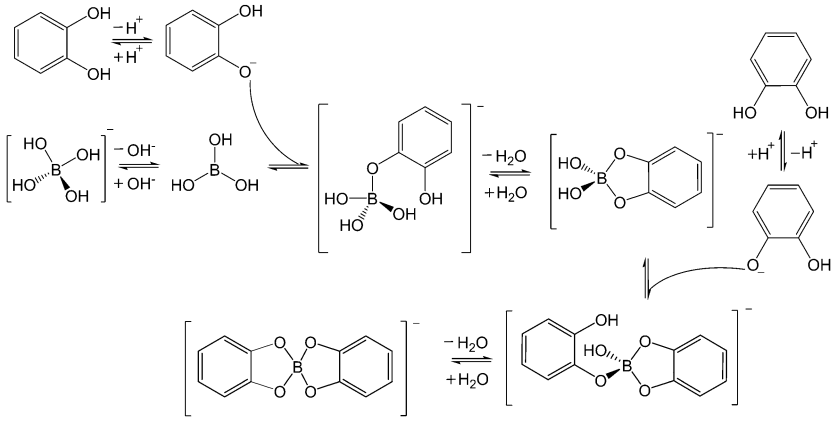

Scheme 1. The equilibrium reaction of H_3BO_3 with catechol in water.

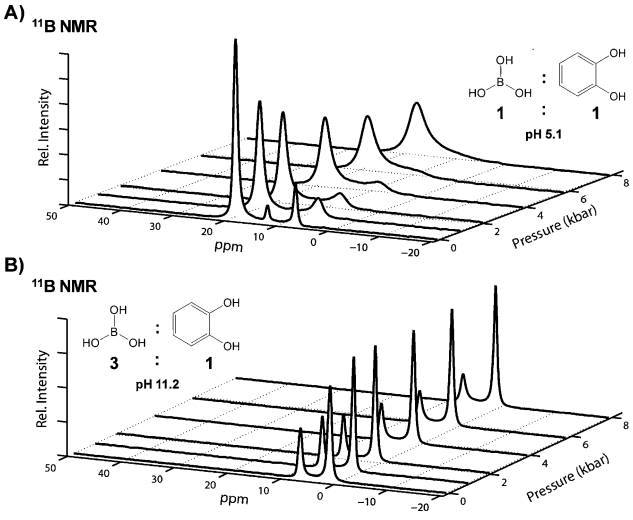

Figure 2. Stacked ^{11}B NMR spectra as a function of pressure: A) A solution containing H_3BO_3 (0.3 M) and catechol (0.3 M) adjusted to pH 5.1 with NaOH (0.5 M). The gradual broadening and coalescence of the peaks with increasing pressures suggests that the reaction is undergoing dynamic exchange as ^{11}B sites are becoming equivalent on the NMR time scale. B) A solution containing H_3BO_3 (0.3 M) and catechol (0.1 M) adjusted to pH 11.2 with NaOH (1.0 M). The lines broaden slightly as a function of pressure but do not coalesce.

 © 2014 Wiley-VCH Verlag GmbH & Co. KGaA, Weinheim

Figure SI 6) and observed for all solution compositions tested with an initial pH° 5.1 and catechol concentrations equal to or lower than H_3BO_3 in solution (see Figure SI 5). In solutions where the concentrations of catechol are greater than H_3BO_3 at pH° 5.1, the mono- and bis-catecholate species are more prominent, yet still undergo dynamic exchange and coalescence as pressure increases to 8 kbar (see Figure SI 7). This exchange is the direct result of pressure and not temperature, as variable-temperature experiments between 286–362 K, collected in a conventional 5 mm NMR probe, did not show peak coalescence (see Figure SI 8) or chemical-exchange broadening. The dependence on pressure is expected from the change in boron coordination (trigonal to tetrahedral) that accompanies the reaction, the increased dielectric constant of water and the corresponding changes in solute ionization as described by the Drude–Born–Nernst relation.

When the pH° is adjusted above the pK_a value of both H_3BO_3 and catechol (>10), the solution is dominated by mono-catecholate (7.9 ppm) and free $B(OH)_{4\ (aq)}^-$ (2.9 ppm; Figure 2 B). As pressure increases, each of the signals broaden slightly, but they do not coalesce and dynamic exchange is not evident. This trend is consistent with other solution compositions (see Figure SI 9) and likely indicates that the reactivity of borate ions is much lower than the reactivity of H_3BO_3 with 1,2-diols.[39] Similarly, under acidic conditions (pH° 2.3), the reaction between H_3BO_3 and catechol does not proceed and only a single ^{11}B resonance (free H_3BO_3; 19.2 ppm) is observed at all pressures (see Figure SI 10).

The pressure dependence of the dynamic exchange observed for the samples with original ambient pH° 5.1 allows for the estimation of rate coefficients. Exchange of ^{11}B nuclei between free H_3BO_3 and the mono-catecholate boron complex in solution can be approximated by a pseudo-first-order, two-site exchange model by analytically solving the Bloch equations[40] while adopting the McConnell formalism for exchange (see the Supporting Information for the details).[41] The resulting first-order exchange rate constants are used to calculate the activation volume ($\Delta V^{\neq}$) by the following equation (R is the gas constant, T the temperature, k the rate coefficient, and P the pressure).[42]

$$(\delta \ln k/\delta P)_T = -\Delta V^{\neq}/RT \quad (1)$$

In most studies at lower pressures, a plot of $\ln k$ vs. P yields a linear relationship with a slope of $-\Delta V^{\neq}/RT$. However, if there is a pressure dependence to $\Delta V^{\neq}$, as is expected at these higher pressures, the solution compressibility ($\Delta\beta^{\neq}$) must also be considered.[42,43]

$$(\delta \Delta V^{\neq}/\delta P)_T = -\Delta\beta^{\neq} \quad (2)$$

The apparent activation parameters can be extracted by a plot of $\ln k$ vs. P, and fitted to the quadratic Equation (3).

$$(\ln k^P/k^o) = -(\Delta V^{\neq}/RT)\,P + 0.5(\Delta\beta^{\neq}/RT)\,P^2 \quad (3)$$

The results for four samples where the catechol concentrations are less than H_3BO_3 are shown in Figure 3 (with k_{ex} plotted as a function of pressure shown in Figure SI 11). The

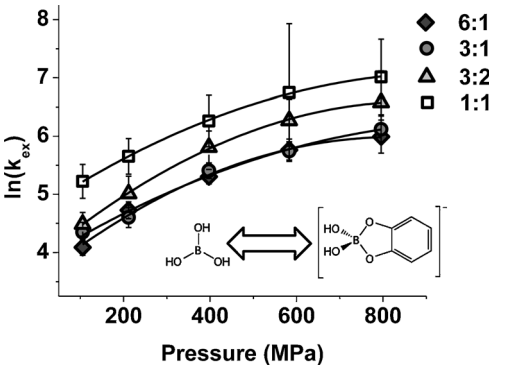

Figure 3. $\ln(k_{ex})$ as a function of pressure for various H_3BO_3 (0.3 M)/catechol solution compositions at $T = 323$ K. The data are fitted to the quadratic Equation (3) with the resulting apparent activation parameters compiled in Table 1. The inset shows the two ^{11}B species used to calculate k_{ex} from the ^{11}B NMR spectra acquired on the high-pressure cell NMR probe. The error bars indicate the standard error of each datum.

apparent $\Delta V^{\neq}$ and $\Delta\beta^{\neq}$ values are reported in Table 1, which suggests that the conversion between the free H_3BO_3 and the mono-catecholate in solution proceeds due to the increase in electrostriction, outweighing any positive contribution to $\Delta V^{\neq}$ by the release of a H_2O molecule during the ring closure,[42] with the caveat that this multi-step exchange process is approximated by the McConnell–Bloch equations. The solution compressibility coefficient, $\Delta\beta^{\neq}$, must be included in all our experimental data; if neglected, the calculated $\Delta V^{\neq}$ parameters would be underestimated by almost half.

Table 1: Apparent activation parameters determined at (323.0 ± 0.1) K.

Sample composition (H_3BO_3/catechol)	$\Delta V^{\neq}$ [$cm^3\,mol^{-1}$]	$\Delta\beta^{\neq}$ [Pa^{-1}]
6:1	−15.4 ± 1.6	−0.019 ± 0.002
3:1	−12.0 ± 2.4	−0.011 ± 0.003
3:2	−16.3 ± 0.6	−0.019 ± 0.001
1:1	−12.0 ± 0.5	−0.013 ± 0.001

This adaptation of the pressure cell enables solution-state NMR experiments at unprecedented pressures. The calibration of the probe up to 20 kbar by in situ ruby fluorescence shift allows for the direct measurement of molecular speciation and dynamics using any NMR-active nucleus in aqueous solutions under pressures that are equivalent roughly to those at the base of the Earth's continental crust, albeit at much lower temperatures. The probe design is inexpensive and provides the ability to examine solution chemistries that were previously inaccessible, including direct interpretation of reaction mechanisms in terms of intrinsic and solvation components up to much higher pressures.[43] This technique is particularly important to the advancement of geochemical goals, such as validating predictions from the newly revised HKF equations for solution thermodynamics at high pressures and temperatures. These also include the speciation and solubility of metals in aqueous solutions,[2,3] but may also be

 © 2014 Wiley-VCH Verlag GmbH & Co. KGaA, Weinheim

extended to multinuclear methods critical to understanding carbon biogeochemical cycling and petroleum formation.

Experimental Section

Aqueous solutions containing H_3BO_3 and catechol were prepared by dissolving the appropriate amounts of each in degassed water in an inert atmosphere to minimize the risk of solution oxidation. The pH of the solutions were adjusted by the addition of 0.5 M NaOH.

The pressure cell was constructed of BeCu[25] and adapted to include a resonance circuit (see Figure SI 1 for a picture of the entire probe). The device was equipped with a copper (for experiments up to 8 kbar) or phosphor bronze (for experiments above 8 kbar) solenoid microcoil (3.5 mm diameter) in the sample space with electrical leads fed through a hole in the center and sealed with Stycast 2850FT.[25,26] Boron-catechol samples ($\approx$10 μL) were pipetted into PEEK tubing (2.5 mm diameter, 0.05 mm wall), sealed with epoxy and placed within the microcoil. The microcoil containing the sample was inserted into a Delrin cap filled with an inert pressure-transfer fluid oil (Halocarbon 6.7). This was loaded into the pressure cell containing a BeCu (for experiments up to 8 kbar) or tungsten-carbide (for experiments above 8 kbar) piston. A hydraulic pump is used to apply the external pressure, and the internal pressure is calibrated via in situ ruby fluorescence and a fiber optic fed through the plug, with a diode-pumped solid-state green laser (532 nm) and monitored with a charge-coupled device spectrometer (Figure SI 2).[26]

High-pressure ^{11}B NMR measurements were acquired on a wide-bore Bruker Avance 400 MHz (9.4 T) spectrometer (8192 scans) with calibrated a $\pi/2$ pulses (10 dB attenuation from the 300 W broadband amplifier: 30 W) and a relaxation delay of 0.05 s. Sample T_1 measurements were performed on a 0.05 M H_3BO_3 sample using an inversion–recovery pulse program, and dropped from 8.2 ms under ambient conditions to 7.1 ms at 8 kbar. Hahn-echo experiments for T_2 performed on the 0.05 M H_3BO_3 sample increased from 3.1 ms under ambient conditions to 5.5 ms at 8 kbar. The temperature of the probe (40 °C for experiments up to 8 kbar, 60 °C for experiments up to 20 kbar) was controlled with a heated water bath to prevent pressure-induced freezing,[44] monitored by a thermocouple and allowed to equilibrate after each pressure change (20–30 min). Spectra were reacquired at ambient conditions after pressurization to ensure that changes were reversible. The ^{11}B chemical shifts were referenced to the $H_3BO_3/NaBO_4$ equilibrium.[29]

Received: May 5, 2014
Published online: July 2, 2014

Keywords: geochemistry · high-pressure NMR spectroscopy · NMR probe design · reaction kinetics

[1] E. L. Shock, E. H. Oelkers, J. W. Johnson, D. A. Sverjensky, H. C. Helgeson, *J. Chem. Soc. Faraday Trans.* **1992**, *88*, 803.
[2] D. A. Sverjensky, B. Harrison, D. Azzolini, *Geochim. Cosmochim. Acta* **2014**, *129*, 125.
[3] D. Pan, L. Spanu, B. Harrison, D. A. Sverjensky, G. Galli, *Proc. Natl. Acad. Sci. USA* **2013**, *110*, 6646.
[4] M. Mookherjee, H. Keppler, C. E. Manning, *Geochim. Cosmochim. Acta* **2014**, *133*, 128.
[5] N. Zotov, H. Keppler, *Chem. Geol.* **2002**, *184*, 71.
[6] B. O. Mysen, *Am. Mineral.* **2010**, *95*, 1807.
[7] B. O. Mysen, K. Mibe, I. M. Chou, W. A. Bassett, *J. Geophys. Res. [Solid Earth]* **2013**, *118*, 6076.
[8] J. D. Frantz, J. Dubessy, B. O. Mysen, *Chem. Geol.* **1994**, *116*, 181.
[9] S. Facq, I. Daniel, D. A. Sverjensky, *Geochim. Cosmochim. Acta* **2014**, *132*, 375.
[10] G. S. Pokrovski, L. S. Dubrovinsky, *Science* **2011**, *331*, 1052.
[11] C. Schmidt, R. Thomas, W. Heinrich, *Geochim. Cosmochim. Acta* **2005**, *69*, 275.
[12] A. J. Simpson, M. J. Simpson, R. Soong, *Environ. Sci. Technol.* **2012**, *46*, 11488.
[13] J. Jonas, P. Koziol, X. Peng, C. Reiner, D. M. Campbell, *J. Magn. Reson. Ser. B* **1993**, *102*, 299.
[14] L. Ballard, A. M. Yu, C. Reiner, J. Jonas, *J. Magn. Reson.* **1998**, *133*, 190.
[15] M. M. Hoffmann, M. S. Conradi, *Rev. Sci. Instrum.* **1997**, *68*, 159.
[16] R. L. Johnson, S. J. Harley, C. A. Ohlin, A. F. Panasci, W. H. Casey, *ChemPhysChem* **2011**, *12*, 2903.
[17] S. J. Harley, C. A. Ohlin, R. L. Johnson, A. F. Panasci, W. H. Casey, *Angew. Chem.* **2011**, *123*, 4559; *Angew. Chem. Int. Ed.* **2011**, *50*, 4467.
[18] R. L. Johnson, C. A. Ohlin, K. Pellegrini, P. C. Burns, W. H. Casey, *Angew. Chem.* **2013**, *125*, 7612; *Angew. Chem. Int. Ed.* **2013**, *52*, 7464.
[19] M. Lesemann, K. Thirumoorthy, Y. J. Kim, J. Jonas, M. E. Paulaitis, *Langmuir* **1998**, *14*, 5339.
[20] J. Y. Buser, A. D. McFarland, *Chem. Commun.* **2014**, *50*, 4234.
[21] J. Jonas, L. Ballard, D. Nash, *Biophys. J.* **1998**, *75*, 445.
[22] C. E. Munte, M. B. Erlach, W. Kremer, J. Koehler, H. R. Kalbitzer, *Angew. Chem.* **2013**, *125*, 9111; *Angew. Chem. Int. Ed.* **2013**, *52*, 8943.
[23] J. Roche, J. Ying, A. S. Maltsev, A. Bax, *ChemBioChem* **2013**, *14*, 1754.
[24] H. R. Kalbitzer, I. C. Rosnizeck, C. E. Munte, S. P. Narayanan, V. Kropf, M. Spoerner, *Angew. Chem.* **2013**, *125*, 14492; *Angew. Chem. Int. Ed.* **2013**, *52*, 14242.
[25] I. R. Walker, *Rev. Sci. Instrum.* **1999**, *70*, 3402.
[26] K. Koyama-Nakazawa, M. Koeda, M. Hedo, Y. Uwatoko, *Rev. Sci. Instrum.* **2007**, *78*, 066109.
[27] G. J. Piermarini, S. Block, J. D. Barnett, R. A. Forman, *J. Appl. Phys.* **1975**, *46*, 2774.
[28] Z. A. Nalkina, *Izu. Sib. Otd. Akad. Nauk SSSR Ser. Khim. Nauk* **1983**, *2*, 46.
[29] M. Bishop, N. Shahid, J. Z. Yang, A. R. Barron, *Dalton Trans.* **2004**, 2621.
[30] R. K. Momii, N. H. Nachtrieb, *Inorg. Chem.* **1967**, *6*, 1189.
[31] C. G. Salentine, *Inorg. Chem.* **1983**, *22*, 3920.
[32] K. E. Bett, J. B. Cappi, *Nature* **1965**, *207*, 620.
[33] L. Babcock, R. Pizer, *Inorg. Chem.* **1980**, *19*, 56.
[34] R. Pizer, L. Babcock, *Inorg. Chem.* **1977**, *16*, 1677.
[35] L. Babcock, R. Pizer, *Inorg. Chem.* **1983**, *22*, 174.
[36] R. Pizer, P. J. Ricatto, S. Jacobson, *Inorg. Chem.* **1995**, *34*, 1007.
[37] M. Pasdeloup, C. Brisson, *Org. Magn. Reson.* **1981**, *16*, 164.
[38] R. Pizer, P. J. Ricatto, *Inorg. Chem.* **1994**, *33*, 2402.
[39] T. Okamoto, A. Tanaka, E. Watanabe, T. Miyazaki, T. Sugaya, S. Iwatsuki, M. Inamo, H. D. Takagi, A. Odani, K. Ishihara, *Eur. J. Inorg. Chem.* **2014**, 2389 – 2395.
[40] F. Bloch, W. W. Hansen, M. Packard, *Phys. Rev.* **1946**, *70*, 474.
[41] H. M. McConnell, *J. Chem. Phys.* **1958**, *28*, 430.
[42] C. D. Hubbard, R. van Eldik in *Physical Inorganic Chemistry: Principles, Methods, and Models* (Ed.: A. Bakac), Wiley, Hoboken, **2010**, p. 269.
[43] A. Drljaca, C. D. Hubbard, R. van Eldik, T. Asano, M. V. Basilevsky, W. J. le Noble, *Chem. Rev.* **1998**, *98*, 2167.
[44] M. Choukroun, O. Grasset, *J. Chem. Phys.* **2007**, *127*, 124506.

 © 2014 Wiley-VCH Verlag GmbH & Co. KGaA, Weinheim